Preparation and characterization of SnO_2-based composite metal oxides: active and thermally stable catalysts for CH_4 oxidation

Xiang Wang * and You-chang Xie

Institute of Physical Chemistry, Peking University, Beijing 100871, PR China
E-mail: wangx2@seas.upenn.edu

Received 2 February 2001; accepted 14 May 2001

A series of SnO_2-based catalysts modified by Fe, Cr and Mn were prepared by the combination of redox reaction and co-precipitation methods, and applied to catalytic CH_4 oxidation. The modified catalysts show generally higher activity than the unmodified SnO_2. XRD analysis indicates that Fe, Cr and Mn cations could be incorporated into the lattice of rutile SnO_2 (cassiterite) to form solid solution structure. As a result, more reducible and active oxygen species was formed in the samples, as substantiated by the H_2-TPR results. Moreover, the specific surface areas of the modified catalysts are much higher than that of pure SnO_2 and their crystallite sizes are smaller, indicating they are more resistant to thermal sintering. Indeed, the high specific surface areas and the formation of more active oxygen species in the modified samples are believed to be the predominant reasons leading to their enhanced CH_4 oxidation activity. Eventually, it is noted that SnCrO displays not only remarkable CH_4 oxidation activity, but also potent resistance to SO_2 and water deactivation, which makes it a promising catalyst with the potential to be applied in some real CH_4 oxidation processes.

KEY WORDS: catalytic CH_4 oxidation; SnO_2-based catalysts; Fe, Cr, Mn metal oxides; sulfur poisoning

1. Introduction

Catalytic oxidation of CH_4 at low temperature is an effective and promising approach to utilize it as a fuel, or prevent it from emitting into the atmosphere [1–8]. Presently, the most commonly used catalysts for hydrocarbon combustion are noble metals such as Pt, Pd, Rh or their combinations [9,10]. However, these conventional catalysts are reported to still have some drawbacks [3–5]. Moreover, due to the limited source and high price of precious metals [11], over recent years, people paid considerable attention to base metal oxides, expecting to find some promising catalysts. Though much work has been done, to reach the goal, more is needed.

SnO_2 is an n-type oxide and has been intensively studied as gas sensor [12–14]. In contrast, the studies on SnO_2 as catalyst are relatively less, though it has already been tried for quite several reactions, such as SO_2 oxidation [15–17], CO oxidation [18–23], NO_x reduction by CO [24–27] or hydrocarbons [28–30] and CH_3Cl oxidation or decomposition [31]. More recently, SnO_2 was employed as a support for Pt and Pd to prepare catalysts for CO and CH_4 oxidation [8,32–38]. However, a literature survey indicates the absence of investigations on using SnO_2-based composite metal oxides for CH_4 oxidation. Therefore, our first incentive to carry out this work is to probe the possibility of applying this class of catalysts for CH_4 oxidation.

Catalytic CH_4 oxidation is a strong exothermic reaction. Though it proceeds at much lower temperature (below 650 °C) [4,7] than traditional high temperature catalytic combustion of diluted CH_4 to provide energy [9,10], good thermal stability is still necessary for the catalysts to get high activity and maintain long time stable performance. However, single component SnO_2 has been proven to have poor thermal stability and sinter easily at high temperature [13,39]. Furthermore, previous studies show that CH_4 oxidation is diffusion controlled rather than reaction controlled at high CH_4 conversion [40,41]. The specific surface area of a catalyst thus plays a key role to achieve a low CH_4 complete conversion temperature. Therefore, modifying pure SnO_2 with suitable methods to get more stable catalysts that can maintain larger surface areas even at high temperature, and show higher activity than individual SnO_2 is rather desirable. In fact, this is our main objective in the present work. Our results indeed demonstrate that a series of SnO_2-based composite oxides with better thermal stability and higher CH_4 oxidation activity than pure SnO_2 can be prepared by an easy method, namely, the combination of redox reaction and co-precipitation. The catalysts were characterized by means of N_2-BET, XRD and H_2-TPR techniques. The physicochemical properties of the catalysts are discussed and correlated with their activity.

2. Experimental

2.1. Catalyst preparation

The precipitation method as in references [13,19,39] was used to prepare SnO_2 precursor (225 m^2/g). This precursor was then calcined at 600 °C in air atmosphere for ∼6 h

---

* To whom correspondence should be addressed.

to get unmodified SnO_2 catalyst. For comparative study, Fe_2O_3, Cr_2O_3 and Mn_2O_3 were also prepared with the similar method.

The multi-component samples were prepared by the stoichiometric reaction between $SnCl_2$ suspension (1 g $SnCl_2\cdot 2H_2O$/15 ml distilled H_2O) and K_2CrO_4 (0.50 M), $Fe(NO_3)_3$ (0.33 M) or $KMnO_4$ (0.25 M) solutions. The reactions can be described simply with the following equations:

$$3Sn^{2+} + 2Cr^{6+} \rightleftharpoons 3Sn^{4+} + 2Cr^{3+} \quad (1)$$

$$Sn^{2+} + 2Fe^{3+} \rightleftharpoons Sn^{4+} + 2Fe^{2+} \quad (2)$$

$$3Sn^{2+} + 2Mn^{7+} \rightleftharpoons 3Sn^{4+} + 2Mn^{4+} \quad (3)$$

It is noted here that the oxidation states of Fe, Cr and Mn in the real catalysts are more complicated and possibly different from the values shown on the left sides in these equations, since they are subsequently calcined in air atmosphere at 600 °C.

Generally, calculated amounts of these solutions were dripped slowly into the $SnCl_2$ suspension. The white color of the suspension changed quickly into some deep colors, *e.g.*, dark green (K_2CrO_4), yellow ($Fe(NO_3)_3$) or brown ($KMnO_4$), indicating that the redox reaction took place promptly. After reaction, 1 N KOH solution was dripped into the mixtures to make the metal cations precipitate out completely (pH $\approx$ 9.7). Afterwards, the precipitates were vacuum-filtered and washed with distilled water repeatedly, until all of the K^+ and Cl^- were removed, and simultaneously the water passing through the precipitate is neutral. The clean precipitates were then dried at 110 °C overnight and followed by calcination at 600 °C in static air for ~6 h. The catalysts are named by their corresponding components, such as SnFeO, SnCrO, SnMnO, SnFeCrO, SnMnCrO, SnMnFeO and SnMnFeCrO. For a catalyst containing two or three types of metal cations other than Sn, the order of the elements in its name shows the addition sequence of the corresponding solutions into the $SnCl_2$ suspension during the sample preparation. For instance, to prepare SnMnFeCrO, the addition sequence of the solutions into the suspension is first $KMnO_4$, then $Fe(NO_3)_3$, and finally K_2CrO_4. The compositions of the catalysts are listed in table 1.

Table 1
Chemical compositions of the catalysts.

Catalyst	Chemical composition (atomic ratio)			
	Sn	Fe	Cr	Mn
SnO_2	100	–	–	–
SnFeO	33	67	–	–
SnCrO	60	–	40	–
SnMnO	60	–	–	40
SnFeCrO	50	25	25	0
SnMnCrO	60	0	20	20
SnMnFeO	50	25	–	25
SnMnFeCrO	55	15	15	15

2.2. Catalyst characterization

The specific surface areas of the samples were measured by nitrogen adsorption–desorption at 77 K with an ST-30 instrument.

XRD patterns were recorded on a BD-90 X-ray diffractometer with Cu K_α radiation of 40 kV × 20 mA and Ni filter. For phase composition analysis, the scan step is 0.1° with a preset counting time of 4 s. For mean crystallite size measurement, the scan step is 0.01° with a preset counting time of 4 s. The crystallite sizes of the samples were evaluated from the broadening of the strongest peak of SnO_2, peak (110), and based on Scherer equation after necessary correction.

H_2-TPR experiments were carried out with a H_2/N_2 (5.1%) gas mixture, the temperature being increased from room temperature to 800 °C with a ramp of 10 °C/min. Generally, 50 mg catalysts were used and a thermal conductivity detector (TCD) was employed to monitor the H_2 consumption. Prior to the experiment, the samples were calcined again in dry air at 600 °C for 1 h, then cooled down to room temperature, and followed by purging with a high purity N_2 flow for ~30 min.

2.3. Catalytic evaluation

Catalytic tests were carried out in a U-shaped fixed-bed microreactor (ID $=$ 6 mm) with a continuous downflow. The samples were pressed under 8 MPa for 2 min to form pellets, and then crushed and sieved. Typically, 0.2 ml 40–60 mesh catalysts were used for activity evaluation. To avoid channeling, ~1 ml porcelain particles with same size were loaded above the catalyst bed. A blank experiment showed the lack of activity of these porcelain particles at the reaction temperature region. A K-type thermocouple was placed on top of the catalyst bed (touched the catalyst) to monitor the reaction temperature. To measure the light-off behaviors of the catalysts, all data were collected with ascending the temperature. The volume composition of the feed gas is CH_4 1.5%, O_2 18% and balanced by high purity N_2. The total feed flow rate was 70 ml/min corresponding to a gas hourly space velocity (GHSV) of 21,000 h^{-1}. The reactants and products were analyzed with an on-line 1102G GC equipped with a TCD on Porapak Q column for CH_4 and CO_2, and on molecular sieve 5A column for CH_4 and CO. Before analysis, the reaction at each temperature over all studied catalysts was stabilized at least 30 min. To obtain reproducible and stable results, generally, 3–5 injections were made for each point. The flow rate of the carrier gas He is 30 ml/min. CH_4 conversion was calculated by the change of its peak area before and after the catalyst bed.

3. Results

3.1. Activity evaluation

The light-off curves of CH_4 oxidation over the catalysts are shown in figure 1. For clarity, T_{10}, T_{50} and T_{98}, which are the temperatures corresponding to 10, 50 and 98% CH_4 conversion, are also listed in table 2. For comparative study, the three temperatures of individual Fe_2O_3, Cr_2O_3 and Mn_2O_3 are also included here. In this work, T_{98} is regarded as the CH_4 complete conversion temperature.

Compared with SnO_2, an interesting observation is that the light-off curves of the multi-component samples shift, more or less, to obviously lower temperature region, especially below 480 °C (figure 1). T_{10}, T_{50} and T_{98} of SnO_2 are 370, 440 and 520 °C, respectively. In contrast, the three temperatures of individual Fe_2O_3, Cr_2O_3 and Mn_2O_3 are generally higher than those of SnO_2. However, all the multi-component samples show lower T_{10} and T_{50} than SnO_2; and most of the samples exhibit also lower T_{98} except SnFeO and SnMnO. SnMnFeO displays the best reaction activity among all the catalysts, with the CH_4 complete conversion temperature as low as 470 °C.

The CH_4 oxidation rates of all the catalysts measured at 340 °C are also included in table 2. At this temperature, stable CH_4 conversion on most of the catalysts is below 10%, except that on SnCrO and SnMnO is 13 and 15%, respectively. The rates based on per gram catalyst of those multi-component catalysts are much higher than that of pure SnO_2 and individual Fe_2O_3, Cr_2O_3 and Mn_2O_3. The rates normalized by specific surface area of part of the catalysts are also listed in the table. Most of the measured multi-component catalysts show similar values to SnO_2 and lower values than Fe_2O_3, Mn_2O_3 and Cr_2O_3 due to their higher surface areas, while the rate on SnCrO is still much higher than that on the pure oxides. Clearly, the incorporation of Fe, Cr or Mn cations into SnO_2 can enhance the activity of the achieved catalysts. However, it is mentioned here that the activity of these SnO_2-based composite oxides is still lower than that of supported Pd catalysts [34].

The catalysts were thus subjected to sulfur poisoning test at their corresponding T_{98}, with the results on SnCrO and SnFeO shown in figure 2. First, we ran the reaction 2–3 h at the due temperature until the CH_4 conversion was stabilized. Then we began to inject pure SO_2 into the reaction feed (1 ml/injection) with an interval of 20 min. Apparently, SnFeO was severely deactivated by SO_2. The first injection

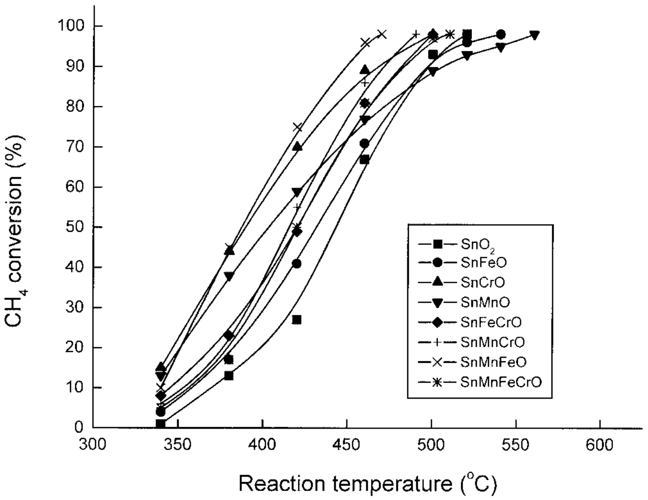

Figure 1. Light-off curves of CH_4 oxidation over pure SnO_2 and SnO_2-based composite oxide catalysts. Data were collected in a flow of 1.5% CH_4, 18% O_2 and N_2 balance with a GHSV of 21,000 h^{-1} and total pressure of 1 atm.

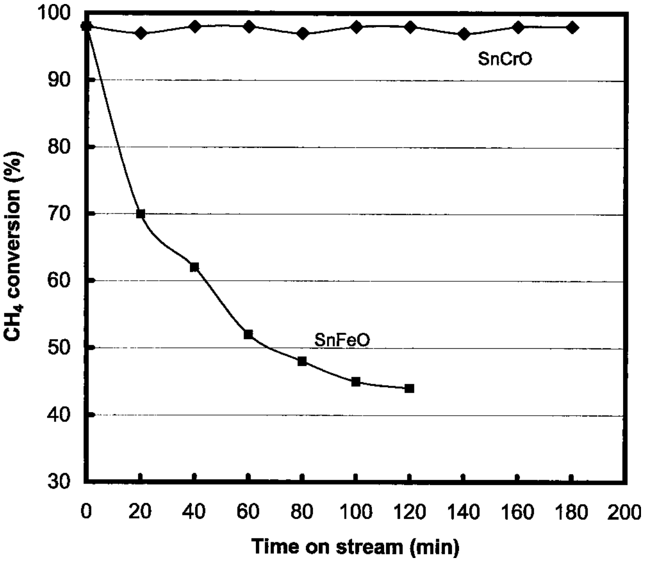

Figure 2. SO_2 poisoning tests of SnFeO and SnCrO. Data were collected in a flow of 1.5% CH_4, 18% O_2 and N_2 balance with a GHSV of 21,000 h^{-1} and total pressure of 1 atm. SO_2 was injected into the flow with an interval of 20 min (1 ml/injection). Reaction temperatures 540 °C for SnFeO and 500 °C for SnCrO.

Table 2

Comparison of the CH_4 oxidation activity on the catalysts.

Catalyst	SnO_2	SnFeO	SnCrO	SnMnO	SnFeCrO	SnMnCrO	SnMnFeO	SnMnFeCrO	Fe_2O_3	Cr_2O_3	Mn_2O_3
T_{10}[a] (°C)	370	350	320	325	345	350	340	360	370	415	375
T_{50}[b] (°C)	440	420	390	405	420	415	385	420	455	500	420
T_{98}[c] (°C)	520	540	500	560	500	490	470	500	570	>600	575
Reaction rate[d] ($\times 10^{-5}$ mmol/s g)	2.2	6.7	29.0	33.5	8.9	13.4	22.3	11.2	5.8	2.0	6.3
Reaction rate[d] ($\times 10^{-7}$ mmol/s g)	7.7	8.3	41.3	–	6.0	–	–	7.2	23.2	20.0	27.4

[a] Temperature at which CH_4 is converted 10%.

[b] Temperature at which CH_4 is converted 50%.

[c] Temperature at which CH_4 is converted 98%.

[d] Measured at 340 °C (CH_4 conversion $<15\%$).

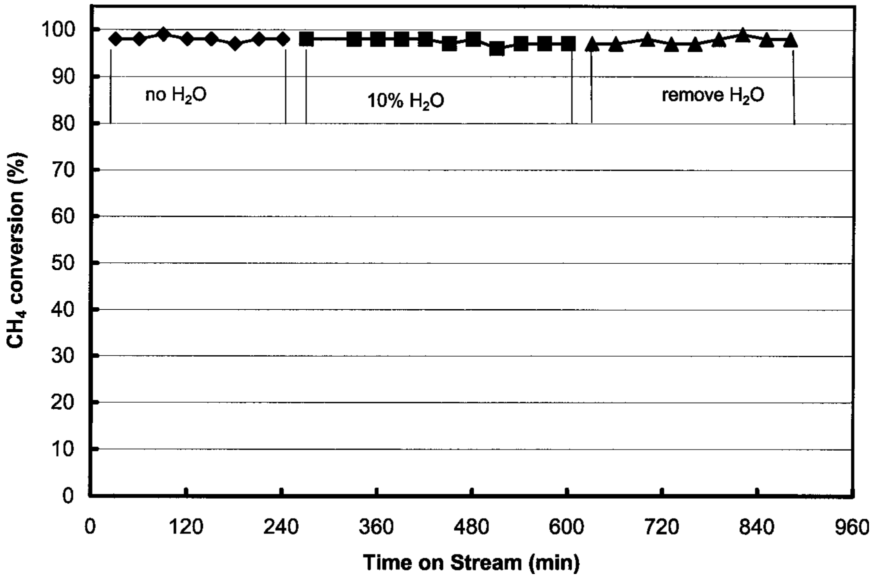

Figure 3. Durability test of SnCrO in the absence and in the presence of 10% water. Data were collected in a flow of 1.5% CH_4, 18% O_2 and N_2 balance with a GHSV of 21,000 h^{-1} and total pressure of 1 atm. Reaction temperature 500 °C.

degraded its CH_4 conversion from 98 to 70%. After five injections, its CH_4 conversion was decreased to ~43%. It is noted here that SO_2 poisoning also occurred to other samples containing Fe and Mn, *e.g.*, SnMnFeO and SnFeCrO. This may be caused by the formation of Mn and Fe sulfates. Surprisingly, SnCrO exhibited potent resistance to sulfur deactivation; nine injections of totally 9 ml SO_2 during ~3 h run have no any negative effect on its activity.

Generally, in real after treatment applications, 5–20% water vapor is present. Therefore, the durability of SnCrO was further evaluated in the presence and in the absence of 10% water at 500 °C, with the results shown in figure 3. First, we ran the reaction in dry feed for ~4 h. Then 10% water was added into the feed through a water saturator. After ~6 h test, water was removed again from the feed. It is evident water did not deactivate SnCrO, demonstrating that it is a stable catalyst.

3.2. XRD and N_2-BET analysis

XRD results of the catalysts are illustrated in figure 4. In unmodified SnO_2, only sharp and high intensity peaks of rutile SnO_2 (cassiterite) are detected, indicating it crystallized very well during the 600 °C calcination. In contrast, in the XRD patterns of those multi-component samples, typically, two or three broadened peaks with very low intensity are observed. Careful analysis demonstrates that these peaks belong also to rutile SnO_2 (cassiterite). It is apparent that the incorporation of Fe, Cr and Mn into tin oxide impeded the crystallization of the prepared samples, thus making the catalysts remain nearly amorphous even at high temperature. Interestingly, though the contents of Fe, Cr and Mn in these samples are high (table 1), no any peak relating to these elements is obviously observed. Two possible reasons could be responsible for this phenomenon: (1) Fe, Cr and Mn oxide dispersed highly on the surface of SnO_2; (2) Fe, Cr and Mn cations doped into the crystal lattice of SnO_2 to form solid solution.

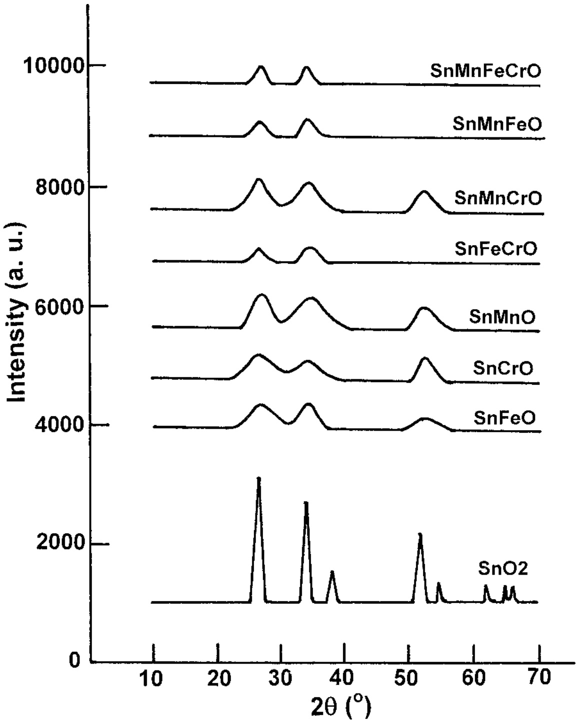

Figure 4. XRD patterns of pure SnO_2 and SnO_2-based composite oxide catalysts.

In this group, Xie *et al.* [42–44] found that a metal oxide can disperse spontaneously onto the surface of another one as a support to form a monolayer, which can significantly increase the thermal stability of both components and impede their crystallization at high temperature. As a result, the supported metal oxide can escape the detection of XRD due to its highly dispersed form as a monolayer. On studying SnO_2

as gas sensor, the same stabilization effects of various metal oxides on SnO_2 were found by Xu *et al.* [39] and Zhao and co-workers [13]. They substantiated that the dispersion of a series of metal oxides, such as CaO, La_2O_3, MgO, *etc.* on ultrafine SnO_2 powder can retard the decrease of the specific surface areas and impede the growth of the crystallite sizes of the achieved samples. Zhao and co-authors ascribed the reason to the formation of metal oxides dispersed as monolayer and submonolayer on the surface of SnO_2 [13].

It is noted here that, in their studies, the samples were prepared by incipient wetness impregnation method and the loading of the supported metal oxides is low. Hence, the metal oxides incline to disperse on the surface of SnO_2 [13,42]. However, in the present work, the catalysts were synthesized *via* redox reactions followed by co-precipitation. The amount of Fe, Cr and Mn oxides in the multi-component samples is high (table 1), and much higher than the general monolayer dispersion capacity [13,42]. Therefore, there is a possibility that the different components in the samples admix into each other in bulk. Moreover, it is noted here that the 2θ of the second (33.8°) and third (51.8°) strongest peaks of rutile SnO_2 phase in pure SnO_2 shift to higher values in the multi-component samples. We thus incline to believe that the low crystallinity of the multi-component samples in this work and the evasion of XRD detection of Fe, Cr and Mn oxides are not mainly due to the formation of monolayers on the surface of SnO_2, but could be due to the second reason, the doping of Fe, Cr and Mn cations into the crystal lattice of rutile SnO_2 [45].

To further testify our assumption, the following strategy was used. SnFeO and SnCrO were calcined at different temperatures higher than 600 °C, then subjected to XRD analysis (figure 5 (A) and (B)). If Fe, Cr and Mn oxides simply dispersed finely on the surface of SnO_2 or merely mixed physically with SnO_2, they are supposed to segregate out and detected by XRD at high enough calcination temperature at which the surface area of SnO_2 becomes very low, and the crystallinity of the oxides is very high [20,46]. However, the main change observed for the samples is that their diffraction peaks become sharper and more intensive upon increasing the temperature, and some new peaks appeared. Rutile SnO_2 is still the only detected crystalline phase. It is worth noting here that the same phenomenon was also observed for SnMnO and SnFeCrO (results not shown). Indeed, this observation indicates that stable structure was formed between Fe, Cr, Mn and Sn oxides. This experiment provided additional proof to testify the formation of solid solution structure in the multi-component samples.

Whereas, the present results are somewhat different from what was found by Harrison *et al.* [46]. On studying Sn–Cr binary oxide catalysts with similar chemical composition and prepared by co-precipitation, as in this study, they found that rutile SnO_2 is the only crystalline phase at low calcination temperature. However, when the catalyst was calcined at 1000 °C, they observed the separation of Cr_2O_3 from SnO_2. Therefore, they excluded the possibility of forming solid solution structure between the two components. This difference could be caused by the different methods used for sample preparations in these two pieces of work, as in our case the method used is actually the combination of redox reaction and co-precipitation. Indeed, our XRD results suggest that Fe, Cr and Mn cations could be doped into the lattice of SnO_2 to occupy some positions of Sn^{4+}, thus leading to the formation of solid solution structure. It is conceivable that the introduction of impurity into the lattice of SnO_2 can impede the mobility of Sn cations during the calcination, thus hinder the crystallization of the prepared samples at high temperature.

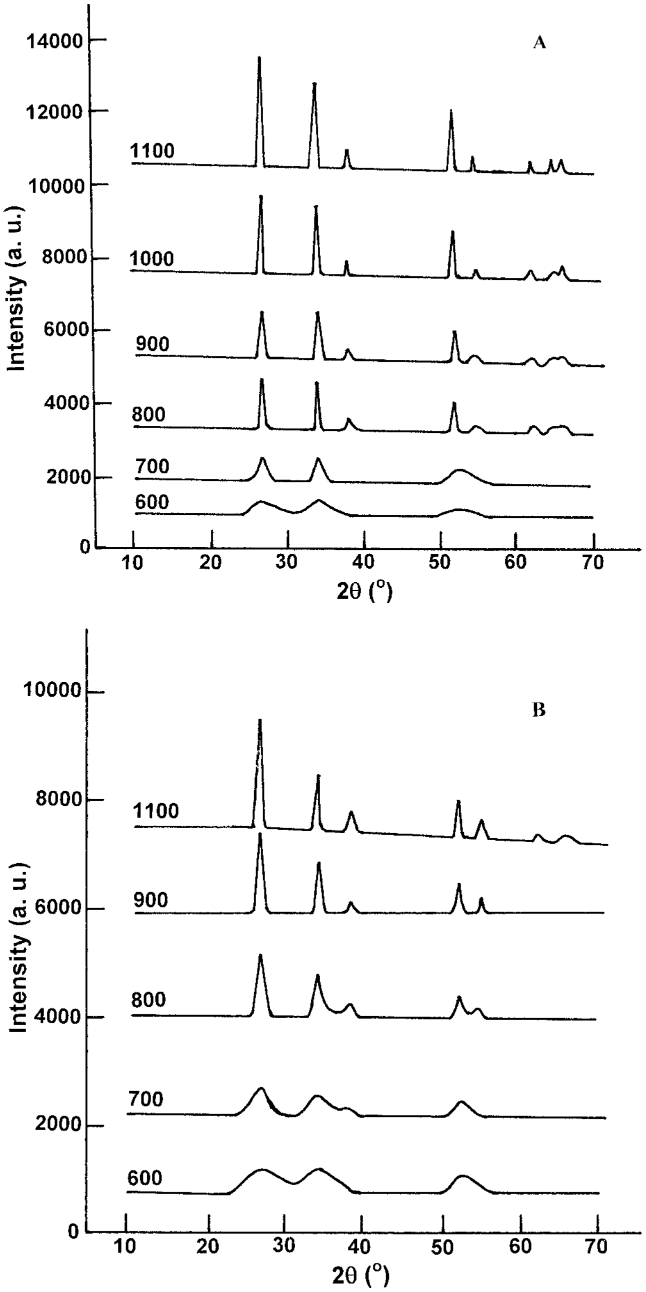

Figure 5. XRD patterns of (A) SnFeO and (B) SnCrO calcined at different temperatures.

Since all of the samples show the diffraction feature of rutile SnO_2, to compare their crystallinity quantitatively, their

Table 3
Specific surface areas and crystallite sizes of the catalysts.[a]

Catalyst	SnO_2	SnFeO	SnCrO	SnMnO	SnFeCrO	SnMnCrO	SnMnFeO	SnMnFeCrO
Crystallite size (Å)	159	45	53	37	40	42	33	36
BET surface area (m^2/g)	291	81	71	–	148	–	–	154

[a] All the samples were calcined at 600 °C for ∼6 h in air atmosphere.

crystallite sizes are estimated based on the broadening of peak (110) of SnO_2 (table 3). The crystallite size of SnO_2 is 159 Å, while that of those multi-component samples is always below 53 Å. It is apparent that the multi-component samples are more resistant to thermal sintering than the pure SnO_2 [14,20,46]. In other words, the incorporation of Fe, Cr or Mn cations into SnO_2 can markedly increase the thermal stability of the prepared samples.

The specific surface areas of part of the samples were also measured and listed in table 3. As mentioned above, the surface area of SnO_2 precursor dried at 110 °C is 225 m^2/g, while it decreased drastically to 29 m^2/g after calcination at 600 °C to prepare applied SnO_2 catalyst. This confirms that the thermal stability of pure SnO_2 is poor [13,39]. Its low surface area is in good agreement with its big particle size and high crystallinity. It is mentioned here that the surface areas of individual Fe_2O_3, Cr_2O_3 and Mn_2O_3 are 25, 10 and 23 m^2/g, respectively, after calcination under the same conditions, indicating that they have low thermal stability as well. The surface areas of SnFeO and SnCrO are 81 and 71 m^2/g, respectively, which is much higher than that of the pure oxides. Interestingly, SnMnFeCrO and SnFeCrO have even unexpectedly larger surface areas than SnFeO and SnCrO, with the values of 148 and 154 m^2/g, respectively. The tendency seems to suggest that the introduction of more different kinds of cations into SnO_2 can lead to better thermal stability of the achieved samples.

3.3. H_2-TPR results

H_2-TPR profiles of the samples are shown in figure 6. Pure SnO_2 shows a peak centered at 760 °C, which has been assigned to the reduction of SnO_2 to metallic Sn [29]. However, its broadened and un-symmetric shape implies that it actually consists of more than one peak, which may correspond to more than one stage to reduce Sn^{4+} to Sn^0. In comparison, the reduction profiles of the multi-component samples are much more complicated, and have at least two peaks. A main and common feature of all the multi-component samples is the formation of one or two low-temperature reduction peaks below 400 °C. Simultaneously, the temperatures of the high temperature reduction peaks shifted to lower region. It is difficult to assign the different peaks to some certain species, because in these samples the reduction of Sn, Fe, Cr and Mn oxides overlapped with each other, and the oxidation states of Fe, Cr and Mn in the samples are not unambiguously determined.

Whereas, the most possible oxidation state of Fe, Cr and Mn could be 3+, since under similar calcination conditions to this work, the most stable oxides of them are Fe_2O_3 [47], Cr_2O_3 [48] and Mn_2O_3 [49,50]. Pure Cr_2O_3 has been found un-reducible by H_2 below 800 °C [48,51]. Therefore, the 280 °C peak of SnCrO could be due to the reduction of dissociatively adsorbed oxygen species in it, which is possibly more reactive. In contrast, under the conditions adopted in this study, Fe_2O_3 shows a reduction peak centered at 445 °C, which starts from ∼400 °C [51,52]; and Mn_2O_3, shows a peak at 350 °C, which starts from 300 °C [43,49]. Therefore, for those samples containing Fe and Mn, there is the possibility that the low temperature peaks could be due to the reduction of Fe or Mn oxides. However, we still cannot exclude the presence of dissociatively adsorbed oxygen species in these samples. It is worth noting here that the oxygen species corresponding to the low temperature peaks can also be reduced by CH_4 around 400 °C [53], indicating they could play the role to activate CH_4 in the reaction temperature region. Indeed, these active oxygen species may con-

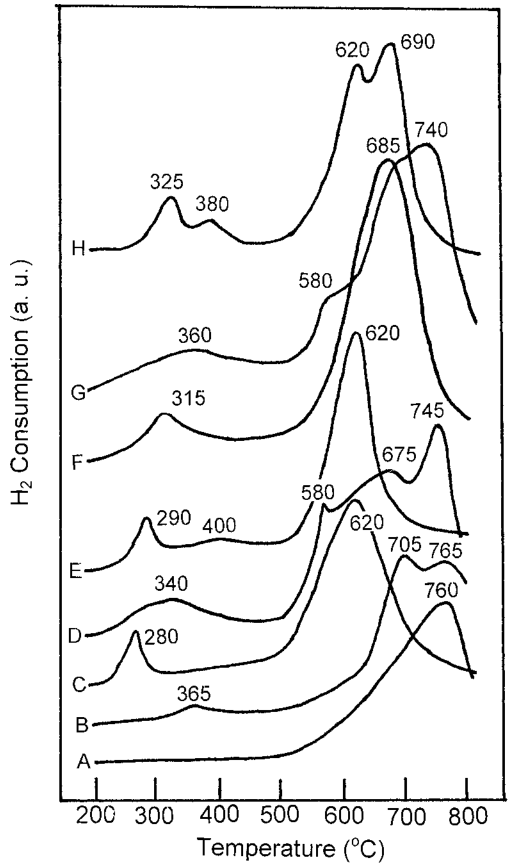

Figure 6. H_2-TPR profiles of the catalysts: (A) SnO_2, (B) SnFeO, (C) SnCrO, (D) SnMnO, (E) SnFeCrO, (F) SnMnCrO, (G) SnMnFeO and (H) SnMnFeCrO.

tribute to the enhanced CH_4 oxidation activity of the multi-component catalysts [1,54,55].

4. Discussion

CH_4 total oxidation is a strong exothermic process, therefore, good thermal stability of a catalyst is favorable for it to achieve high activity and maintain long time durability. Furthermore, it is commonly accepted that this reaction is typically diffusion controlled rather than reaction controlled, especially at high CH_4 conversion. The surface area of a catalyst thus plays a key role for its activity. Over recent twenty years, to get metal oxide catalysts that can maintain high active surface areas even at high temperature for CH_4 oxidation, much endeavor has been made; and various methods have been extensively studied [10,41,55]. An uncommon feature of the multi-component catalysts in the present paper is their much higher surface areas and lower crystallinity than that of the individual components. Indeed, this could be the main reason leading to their enhanced CH_4 oxidation activity.

Previously, it was found that SnO_2 modified by Cu or Cr showed remarkably higher CO oxidation activity than pure SnO_2 [20,56,57]. For these samples, oxygen vacancies on the surface of SnO_2 were observed, which can be replenished by dissociatively adsorbed O_2. As a consequence, some active oxygen species was formed in them, and leading to their improved oxidation activity [20,31,56,57].

In this study, H_2-TPR results also indicate clearly the formation of more reducible and reactive oxygen species in the multi-component samples, as evidenced by the low temperature reduction peaks, and the lower reduction temperatures of the high temperature peaks than that of unmodified SnO_2 (figure 6). The oxygen species corresponding to the low temperature peaks is also reducible by CH_4 at $\sim 400\,^{\circ}\mathrm{C}$ as well [51,53], demonstrating that it can activate CH_4 in the reaction temperature region. The formation of these more active oxygen species in the multi-component catalysts could be due to the incorporation of Fe, Cr and Mn cations, which have probably different oxidation states and radii to Sn^{4+}, into the crystal lattice of rutile SnO_2. As a result, charge imbalance and structure defects take place, which lead to the formation of some sites that can adsorb oxygen dissociatively, and the formation of more active lattice oxygen. Indeed, this is possibly another reason devoting to the enhanced CH_4 oxidation activity of the multi-component catalysts.

5. Conclusion

A series of SnO_2-based catalysts modified by Fe, Cr and Mn was synthesized by the combination of redox reaction and co-precipitation methods. It is found that Fe, Cr and Mn cations could be doped into the crystal lattice of rutile SnO_2 (cassiterite) to form solid solution structure. As a result, more reducible and mobile oxygen species was formed in the achieved samples. Moreover, the doped catalysts have much higher specific surface areas and smaller crystallite sizes than the unmodified SnO_2, indicating they are more resistant to thermal sintering. Indeed, the higher surface areas and the formation of more active oxygen species in the modified samples are considered as the predominant reasons leading to their enhanced CH_4 oxidation activity. Due to its high activity and potent resistance to SO_2 and water deactivation, SnCrO is a promising catalyst for catalytic CH_4 oxidation, which has the potential to be applied in some real processes.

Acknowledgement

The authors gratefully acknowledge the financial support from the National Science Foundation of China.

References

[1] Y. Li and J.N. Armor, Appl. Catal. B 3 (1994) 275.
[2] J.K. Lampert, M.S. Kazi and R.J. Farrauto, Appl. Catal. B 14 (1997) 211.
[3] K. Fujimoto, F.H. Ribeiro, M. Avalos-Borja and E. Iglesia, J. Catal. 179 (1998) 431.
[4] W.S. Epling and G.B. Hoflund, J. Catal. 182 (1999) 5.
[5] Lj. Kundakovic and M. Flytzani-Stephanopoulos, Appl. Catal. A 183 (1999) 35.
[6] X. Wang and Y.C. Xie, Catal. Lett. 72 (2001) 52.
[7] R. Leanza, I. Rosseti, L. Fabbrini, C. Oliva and L. Forni, Appl. Catal. B 28 (2000) 55.
[8] K. Sekizawa, H. Widjaja, S. Maeda, Y. Ozawa and K. Eguchi, Appl. Catal. A 200 (2000) 211.
[9] R. Burch, D.J. Crittle and M.J. Hayes, Catal. Today 47 (1999) 229.
[10] M.M. Zwinkel, S.G. Jaras and P.C. Menon, Catal. Rev. Sci. Eng. 35 (1993) 319.
[11] M. Shelef and G.W. Graham, Catal. Rev. Sci. Eng. 36 (1994) 433.
[12] S.L. Sharp, G. Kumar, E.P. Vicenzi, A.B. Bocarsly and M. Heibel, Chem. Mater. 10 (1998) 880.
[13] Y. Gao, H.B. Zhao and B.Y. Zhao, J. Mater. Sci. 35 (2000) 917.
[14] C.V. Santilli, S.H. Pulcinelli, G.E.S. Brito and V. Briois, J. Phys. Chem. B 103 (1999) 2660.
[15] V.G. Rienacker and J. Scheve, Z. Anorg. Allg. Chem. B 328 (1964) 201.
[16] J. Scheve and E. Scheve, Z. Anorg. Allg. Chem. B 333 (1964) 143.
[17] Yu. Sheve and A.V. Krylova, Kinet. Catal. (English Transl.) (1970) 215.
[18] M.J. Fuller and M.E. Warwick, J. Chem. Soc. Chem. Commun. (1973) 210.
[19] M.J. Fuller and M.E. Warwick, J. Catal. 29 (1973) 441.
[20] M.J. Fuller and M.E. Warwick, J. Catal. 34 (1974) 445.
[21] P.G. Harrison, C. Bailey and W. Azelee, J. Catal. 186 (1999) 147.
[22] S.K. Kulshreshtha, M.M. Gadgil and R. Sasikala, Catal. Lett. 37 (1996) 181.
[23] G.C. Bond, L.R. Molloy and M.J. Fuller, J. Chem. Soc. Chem. Commun. (1975) 796.
[24] F. Solymosi and J. Kiss, J. Chem. Soc. Chem. Commun. (1974) 509.
[25] F. Solymosi and J. Kiss, J. Catal. 41 (1976) 202.
[26] M.J. Fuller and M.E. Warwick, J. Catal. 42 (1976) 418.
[27] F. Solymosi and J. Kiss, J. Catal. 54 (1978) 42.
[28] M.C. Kung, P.W. Park, D.W. Kim and H.H. Kung, J. Catal. 181 (1999) 1.
[29] P.W. Park, H.H. Kung, D.W. Kim and M.C. Kung, J. Catal. 184 (1999) 440.

[30] J. Ma, Y.X. Zhu, J.Y. Wei, X.H. Cai and Y.C. Xie, Stud. Surf. Sci. Catal. 130 (2000) 617.
[31] F. Solymosi, J. Rasko, E. Papp, A. Oszko and T. Bansagi, Appl. Catal. A 131 (1995) 55.
[32] S.K. Kulshreshtha and M.M. Gadgil, Appl. Catal. B 11 (1997) 291.
[33] K. Grass and H.G. Lintz, J. Catal. 172 (1997) 446.
[34] X. Wang and Y.C. Xie, React. Kinet. Catal. Lett. 72 (2001) 115.
[35] H. Widjaja, K. Sekizawa and K. Eguchi, Chem. Lett. (1998) 481.
[36] H. Widjaja, K. Sekizawa and K. Eguchi, Bull. Chem. Soc. Jpn. 72 (1999) 313.
[37] D.R. Schryer, B.T. Upchurch, J.D. Vannorman, K.G. Brown and J. Schryer, J. Catal. 122 (1990) 193.
[38] L.S. Sun, S.Y. Li and B.L. Li, React. Kinet. Catal. Lett. 62 (1997) 151.
[39] C. Xu, J. Tamaki, N. Miura and N. Yamazoe, Chem. Lett. (1990) 441.
[40] M. Machida, K. Eguchi and H. Arai, J. Catal. 103 (1987) 385.
[41] L.C. Yan and L.T. Thompson, Appl. Catal. A 171 (1998) 219.
[42] Y.C. Xie and Y.Q. Tang, Adv. Catal. 37 (1990) 1.
[43] X. Wang and Y.C. Xie, React. Kinet. Catal. Lett. 71 (2000) 3.
[44] X.Y. Wang, B.Y. Zhao, D.E. Jiang and Y.C. Xie, Appl. Catal. A 188 (1999) 201.
[45] F. Okada, A. Satsuma, A. Furuta, A. Miyamoto, T. Hattori and Y. Murakami, J. Phys. Chem. 94 (1990) 5900.
[46] P.G. Harrison, N.C. Lloyd, W. Daniel, C. Bailey and W. Azelee, Chem. Mater. (1999) 896.
[47] M. Baldi, V.S. Escribano, J.M.G. Amores, F. Milella and G. Busca, Appl. Catal. B 17 (1998) L175.
[48] N.E. Fouad, H. Knözinger and M.I. Zaki, Z. Phys. Chem. 186 (1994) 231.
[49] X. Wang and Y.C. Xie, React. Kinet. Catal. Lett. 70 (2000) 43.
[50] E.R. Stobbe, B.A. De Boer and J.W. Geus, Catal. Today 47 (1999) 161.
[51] X. Wang, Ph.D. thesis, Peking University (1998).
[52] X. Wang and Y.C. Xie, React. Kinet. Catal. Lett. 72 (2001) 229.
[53] X. Wang and Y.C. Xie, Chem. Lett. (2001) 216.
[54] H. Kung and M. Kung, Adv. Catal. 33 (1984) 159.
[55] T. Seiyama, Catal. Rev. Sci. Eng. 34 (1992) 281.
[56] P.G. Harrison, C. Bailey, W. Daniel, D. Zhao, I.K. Ball, D. Goldfarb, N.C. Lloyd, C. Bailey and W. Azelee, Chem. Mater. (1999) 3643.
[57] P.B. Fabritchnyl, N.R. Sudakova, V.V. Berentsveig, G. Demazeau, M.I. Afanasov and J. Etourneau, J. Mater. Chem. 2 (1992) 763.